**Current Development in Oceanography**
Volume 1, Number 3, 2010, Pages 173-198
Published Online: February 14, 2011
This paper is available online at http://pphmj.com/journals/cdo.htm


# A SIMPLIFIED UNDERSTANDING FOR CYCLONES IMPACTS ON THE GENERATED WAVE ENERGY SPECTRUM FOR COASTAL AREAS WITH DIFFERENT BOUNDARY CONDITIONS

**M. A. KHALIFA**

(Coastal and Port Engineering Specialist, PhD, Civil Eng.)
20 El - Lahoun St. - Zezinea
Alexandria - Egypt

**Abstract**

Many studies are carried out to handle the generated wave energy due to wind blowing through the different cyclonic activities. Little of them is handle the prediction of this generated energy based on a certain cyclone with specific characteristics. In this research, it concentrates on simplifying the understanding of the main concepts of the spectral analysis of wave energy prediction through a detailed numerical modeling study. The study handles two different practical cases with different characteristics. The first one handles the generated wave energy on four selected observation points on the Egyptian northern coast under both moderate and strong cyclonic conditions for a total expected cyclonic period of 130 hours. The second case handles analyzing this energy for a closed bay area close to the southern boundary of the Atlantic Ocean in South America continent via a constant increasing in time increment effect in the cyclone development for a total time equals 24 hours.

Keywords and phrases: wind cyclones, cyclones impact, generated energy from wind, wave spectrum, coastal areas boundary conditions.

Communicated by Hyo Choi

Received September 23, 2010; Revised October 12, 2010

The study comes up with a group of practical conclusions for the studied cases, which may help to simplify the understanding of the effects of the cyclonic activities on the generated spectral wave energy for coastal areas with different boundary conditions. Therefore, it may be a step forward towards better practical applications in both engineering and research fields.

## 1. Introduction

Ocean waves are produced by the wind. The faster the wind, the longer the wind blows, and the bigger the area over which the wind blows, the bigger the wave height and so the generated energy. The wind speed is considered bigger than the wave speed. They usually result from the wind blowing over a vast enough stretch of fluid surface. Some waves in the oceans can travel thousands of miles before reaching land. Wind waves range in size from small ripples to huge waves. When directly being generated and affected by the local winds, a wind wave system is called a *wind sea*. After the wind ceases to blow, wind waves are called *swell*. More generally, a swell consists of wind generated waves that are not or hardly affected by the local wind at that time. They have been generated elsewhere, or some time ago (Hasselmann [1]) and (CERC [2]).

Theoretically, waves develop till their speed becomes equal to the one of wind. For the energy spectrum, the directional spreading of waves is not included in the wave field description. Including the directional spreading is an important factor for the wave energy spreading distribution determination. Wave spectrum is very important to be determined for a certain wave field classification. The reason is that many different wave fields may have the same statistical characteristics as the significant wave height $(H_s)$ and period $(T_s)$. This makes such characteristics not enough to define a certain wave field (Darbyshire [4]) and (Hasselmann [1]). The spectrum gives the distribution of wave energy among different wave frequencies of wave-lengths on the sea surface. The concept of a spectrum is based on work by Joseph Fourier (1768 - 1830), who showed that almost any function of time $\zeta(t)$ can be represented over the time interval $(-T/2 < t < T/2)$ as the sum of an infinite series of sine and cosine functions with harmonic wave frequencies. Wave spectrum is considered as a big group of Sinusoidal waves accumulated over each others. These Sinusoidal waves propagate in the different directions. There are many known

types of known determined wave spectrum. The most common ones are Pierson-Moskowitz wave spectra and JONSWAP (JOint North Sea WAve Project) spectra. Therefore, the wave spectrum is considered as the fingerprint for a certain wave field (Darbyshire [4]).

## 2. Cyclones Formation and Direction Wave Spectrum

### 2.1. Cyclones formation and energy generation

A cyclone is an area of closed, circular fluid motion rotating in the same direction as the Earth. This is usually characterized by inward spiraling winds that rotate counter clockwise in the Northern Hemisphere and clockwise in the Southern Hemisphere of the Earth as a result of the Coriolis effect. Most large-scale cyclonic circulations are centered on areas of low atmospheric pressure. A cyclone's track is guided over the course of its 2 to 6 day life cycle by the steering flow of subtropical jet stream. Weather fronts separate two masses of air of different densities and are associated with the most prominent meteorological phenomena (Longuet-Higgins [5] and Wikimedia [6]).

They form west of the circulation center and generally move from west to east. They move pole ward ahead of the cyclone path. Occluded fronts form late in the cyclone life cycle near the center of the cyclone and often wrap around the storm center. Waterspouts can also form meso-cyclones, but more often develop from environments of high instability and low vertical wind shear. There are a number of structural characteristics common to all cyclones. As they are low pressure areas, their center is the area of lowest atmospheric pressure in the region. Generally, the effects of the cyclone arrive to the forecast point with a certain pressure (certain radius). The energy rays are independent on wind field. In some cases, the energy travel rays become not continuous to the shoreline, as the simulation time is not enough to cover all the simulated fetch. The ray length is in a direct relation to the energy development. In this case, more simulation time is required. The length of the cyclone wind speed vector represents this speed in the different stages. The energy of the sea (extreme sea conditions) increases rapidly with wind speed with a mathematical relation proportional to its fourth power. The amplitude of wave height increases with a mathematical relation proportional to the third power of the wind speed. This property makes storms so unexpectedly destructive (Komen [7]) and (Wikimedia [6]).

### 2.2. Directional wave spectrum

The unidirectional spectrum (1-D) is integrated over directions from the two directional (2-D) frequencies. The directional spectrum is known as $E(f, \Theta)$, where $(f)$ represents the wave frequencies and $(\Theta)$ represents the directional spreading angle of waves. Figure 1 presents an example for typical distribution for wave directional spectrum as relationship among wave energy densities, frequencies and direction (Goda [8]). As presented, most of energy is traveling in the arrow direction starting from the origin/observation point (path connecting the origin point and the intersection point of energy tracks, which is very close to the maximum energy to occur). The origin point is considered as a representative for the observation location in the field. In general, the energy density spectrum is the sum of the full spectrum integration over the directional domain (full sector from $0^\circ$ to $360^\circ$) (Longuet-Higgins [5]).

## 3. Materials and Methods

### 3.1. The used numerical model for generated wave energy from wind- "DOLPHIN-B1"

DOLPHIN-B1 is a second generation wave model (student version), which is able to predict the wave energy spectra distribution generated from wind. The second generation wave models are developed using varying wind fields and simplified nonlinear interactions. Here, the sea surface is defined as the sum of a large number of individual wave components, each wave propagating with constant frequency according to the linear wave theory. The path of wave components (from origin to the forecast point) is calculated by the conventional methods. After leaving the origin, the wave component interacts with the other wave components. Thus at regular interval of time the energy gained or released in the process can be evaluated till it reaches the forecast point. This procedure can be repeated for a large number of wave components of different frequencies and directions at a given time so that the total energy is obtained at the point of forecast (Digital Hydraulics [9]).

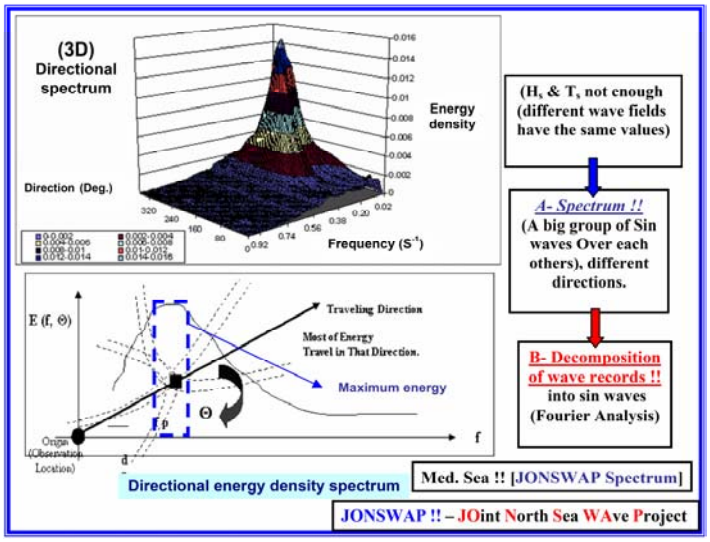


**Figure 1.** Definition sketch for the typical directional energy wave spectrum distribution (Goda [8]).

It is considered as a deep water hybrid point model, a combination of the parametric wind-sea and spectrally treated swells. The development of this model is based on the directionally decoupled energy distribution of wind generated waves. Main inputs to the model are wind field and coastal boundary. Main outputs are significant wave height $(H_s)$, variance density spectra giving information on the two-dimensional distribution of wave energy. By using this model wave parameters are computed over period where observed data is also available. Three hourly values of significant wave height $(H_s)$, zero-crossing period, via many calibration stages for different coastal areas all over the world, the wave spectra predicted by the model and the measured wave spectra seem to be reasonably in good agreement. In the forecast process, the model follows each wave component and determines its energy evolution (Digital Hydraulics [9]).

The used simplified student version is considered simple in numeric but the physical principals are still the same as the full one. These physical processes are called the *source terms*, as presented in equation (1) (Seymour [10], van Vledder [11] and Robert [12]),

$$S = [S_{Wind} + S_{WW-Int.} + S_{WC}], \tag{1}$$

where

$S$ = source term of energy generated by wind,

$S_{Wind}$ = wind source term (feed back mechanism – exponential in growth based on miles),

$S_{WW-Int.}$ = term of wave-wave interaction in deep water (where the wave crests meet),

$S_{WC}$ = term of white capping (dissipation energy).

For $(S_{Wind})$, waves are mainly actively generated by wind. The wind causes energy growth (transfer energy) to the wave spectra. The opposite effect will occur by the white capping as it dissipates energy to the small frequencies, as will be explained after in details. For $(S_{WW-Int.})$, for the case of three wave crests, it called "*triad pattern*" and expressed as $(S_{n/3})$ and the one of four crests is called "*quadruplet pattern*" and expressed as $(S_{n/4})$. For more crests intersection, it is called *diamond pattern*. For the white capping $(S_{WC})$, it is always expressed in a negative sign (as dissipation energy). It has a direct relation to the statistical proportion of white capping via a certain coefficient. This coefficient can be estimated via calibration against wave observation in a certain studied coastal area. It also has a direct proportional relation to wave steepness expressed by mean wave length. The energy transferred by wave-wave interaction (Eg. Quadruplet) to high frequencies is almost totally dissipated by the white capping effect (Narasimhan and Deo [13]).

In DOLPHIN-B1 (student version), two approximations are applied. The first one is for the wave-wave interaction effect. The second is to simulate the effect of wind source term $(S_{Wind})$ and multiply by five to get the effect of both of them, as in equation (2) (Digital Hydraulics [9]),

$$S = [5 * S_{Wind}], \tag{2}$$

$S = 0$, for swell waves.

Significant wave height for a certain wave field can be calculated, as in equation (3),

$$H_s = 4 * \sqrt{M_o}, \tag{3}$$

where $M_0$ = wave energy moment, which is represented as the area under the wave energy distribution curve between $E(f, \theta)$ and $(f)$.

### 3.2. Simplified numerical bases in DOLPHIN-B1 model

The local change of energy for the component $(f, \theta)$ in the mesh comes due to two sources. These sources are both the net import and the local generation of energy. The energy dissipation is considered as negative generation. Figure 2 presents the computational grid and for DOLPHIN-B1 model. The change in energy is as presented in equations (4) through (7),

$$\text{Change in energy} = \frac{\partial E}{\partial t} * \Delta X * \Delta Y * \Delta t, \tag{4}$$

$$\frac{\partial}{\partial X} E(f, \Theta) = -\frac{\partial}{\partial X} E * Cg_x * \Delta X * \Delta Y * \Delta t, \tag{5}$$

$$\frac{\partial}{\partial Y} E(f, \Theta) = -\frac{\partial}{\partial Y} E * Cg_y * \Delta X * \Delta Y * \Delta t, \tag{6}$$

$$\text{Energy local generation} = S * \Delta X * \Delta Y * \Delta t. \tag{7}$$

For more accuracy, the source terms can be expressed in a directional way, as given in the differential equation (8),

$$S(f, \Theta) = \frac{\partial}{\partial t} E(f, \Theta) + \frac{\partial}{\partial X} E(f, \Theta) * Cg_x + \frac{\partial}{\partial Y} E(f, \Theta) * Cg_y \tag{8}$$

where

$\Delta X$ = computational grid unit length,

$\Delta Y$ = computational grid unit width,

$\Delta t$ = computational time interval,

$S(f, \theta)$ = the directional source terms.

$\frac{\partial}{\partial X} E(f, \Theta)$ = net energy import in $(X)$ direction,

$\frac{\partial}{\partial Y} E(f, \Theta)$ = net energy import in $(Y)$ direction,

$(Cg_x)$ and $(Cg_y)$ = wave traveling group velocities in both $(X)$ and $(Y)$ directions, respectively.

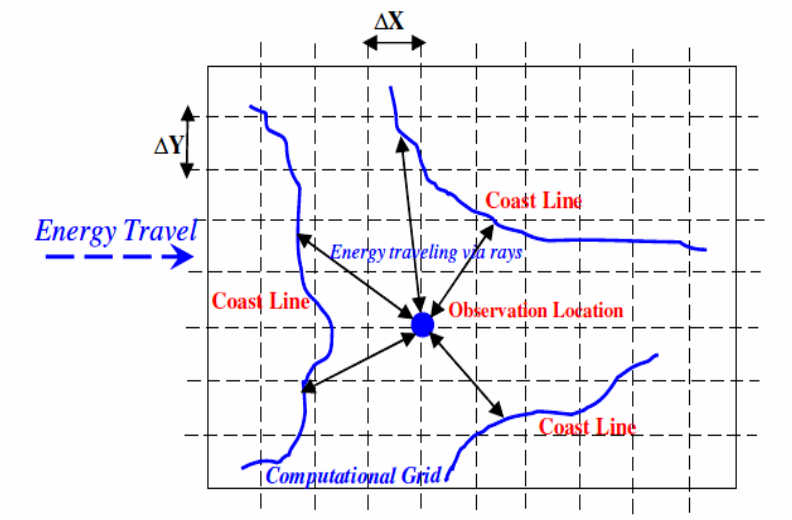


**Figure 2.** Conceptual computational grid and energy traveling paths for DOLPHIN-B1 model.

Both angles of wave energy propagation and local wind field propagation are not compulsory to be the same, but in many cases they are close. The radius of the (2-D) spectrum circle equals the sum of energy around the circle integrated $E(f)$ over $(\theta = 2\Pi)$, as in equation (9),

$$E(f) = \int_0^{2\pi} E(f, \theta)\, d\theta, \tag{9}$$

where

$(\partial\theta) =$ angle of directional spreading (for waves propagation sector).

### 3.3. Wind input

The wind input source term represents the work done by the wind on the ocean surface to produce waves. The wind generation of waves takes place in the high frequency part of the spectrum, i.e., it produces the relatively short waves. The basic theory assumed a linear relationship between wave energy and the rate of change of energy (Narasimhan and Deo [13], CERC [2] and CERC [3]).

According to Miles, the growth rate is dependent on the curvature of the wind profile at the point where the wind velocity equals the wave speed. For positive

values of the growth rate, the wind will give net input of wave energy to the ocean. In the real cases, the growth rate may also have negative values. This means that the flow of energy is from the waves to the wind, i.e., that wave may generate wind. Because waves travel at speeds close to that of wind, the wind is no longer able to transfer energy to them although the sea state has reached its maximum. As the wind speed increases, the waves spectrum grows rapidly while also expanding to the small frequencies (CERC [2], CERC [3] and Stewart [14]).

### 3.4. Dissipation of energy

Wave energy may be lost in two different ways; breaking and frictional dissipation caused by velocity differences. White capping and breaking of waves take energy from the waves and transfer some of it into current. The rest of energy is dissipated, which means that mechanical energy is lost and water is heated up. The wind waves breaking in the deep water is called "*white capping*". This physical process is extremely difficult to model. On the other hand, the dissipation of energy that takes place within the fluid because of velocity differences may be modeled in a way similar to that of wind input, as a linear relationship between the wave energy and the rate of energy change (Thomas et al. [15], CERC [2] and CERC [3]).

### 3.5. Nonlinear wave-wave interaction

If wind input and frictional dissipation were the only process that acting to change the energy spectrum, then ocean waves consist of only short surface waves. When the wave amplitude becomes large, three waves with different lengths may interact through mechanical resonance and create a fourth wave length. Only a limited combination of waves makes this possible.

In this case, most of energy is transferred to the small frequencies and so little energy is transferred to the higher frequencies. This cause dissipation to the wave energy to occur (so, wave energy is shuffled over frequencies). The effect in wave energy over time by both white capping and wave-wave interaction effects is known as overshoot energy. This gives the difference between both Hasselman spectral wave energy mechanism and then real wave spectra energy.

## 4. The Handled Two Case Studies

### 4.1. Case study-no. (1): Egyptian northern coast

Egypt has a quite long coastal stretch on the Mediterranean Sea, which is close

to 200 km in length in the northern boundary, as presented in Figure 3. This coastal stretch is close to be straight. Four observation points (points 1 to 4) were carefully selected along this coast to study the different effects of the generated wave spectral energy variation, as presented in Figure 4. Two runs were carried out by using the student version of DOLPHEN model. The first one considered a moderate cyclonic pressure and the second one considered a quite high pressure one for a total cyclonic period of 130 hours for both of them. In the two cases, the cyclone turns in a clockwise direction and moves from west towards east. The main inputs are presented as in Appendix (A.1). Appendices (A.2) and (A.3) present the inputs for the two studied cases, respectively.

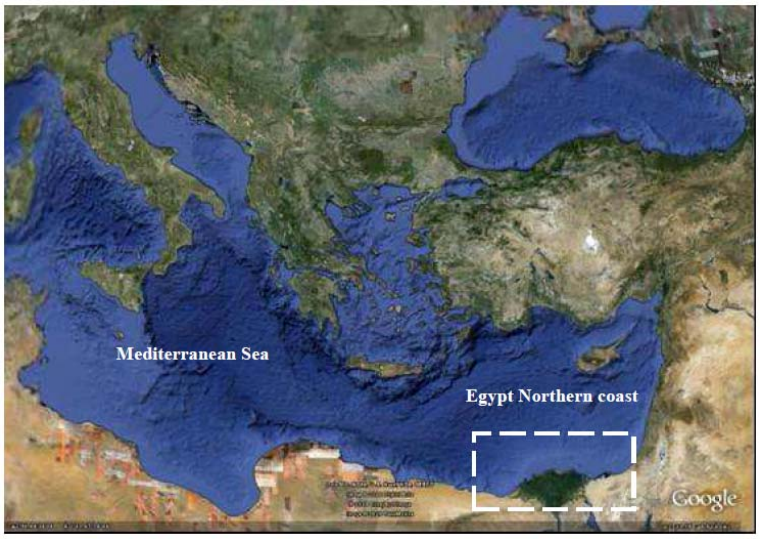


**Figure 3.** Study domain for case No. (1)-The Egyptian northern coast on the Mediterranean Sea (after Google Earth).

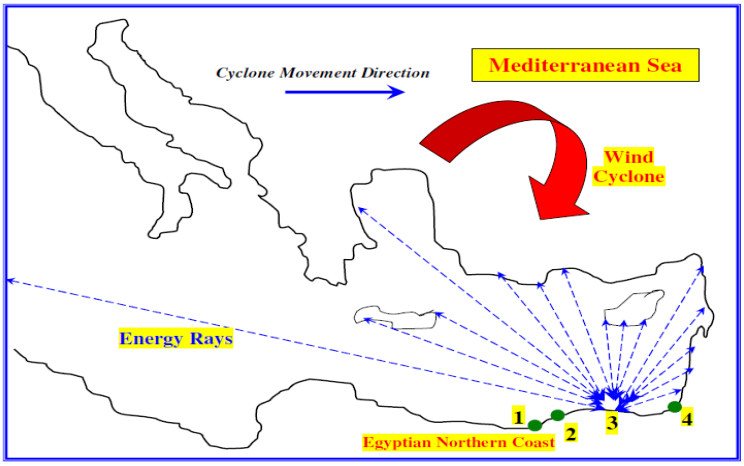


**Figure 4.** Energy rays for location no. (3), on the northern coast of Egypt.

Figures 5.1 through 5.4 present the generated wave energy spectrum from (Dolphin - B1) results for observation location No. (1) through (4)-Egypt northern coast for the high cyclonic pressure conditions, respectively (Ministry of transport-Egypt [18]) and (Admiralty Publications [19]). In these figures, the (2-D) spectrum represents the levels of energy density distributed over frequencies and directions, $E(f, \theta)$ were determined. The (2-D) spectrum is the unidirectional/normalized energy spectrum (1-D) integrated over the angle $(\theta)$, where $(\theta)$ is the angle of wave energy propagation.

Considering the moderate conditions case, the generated wave energy spectrum distributions are considered homogenous for the considered four observation location numbers (1) through (4). The energy contour levels distributions are considered close in both formation and area for observation location numbers (1) and (4). Same conditions are also existed for the observation location numbers (2) and (3). The wave propagation angle $(\theta)$ values are considered close for all locations. The angles of directional spreading $(\partial\theta)$ are considered close for all studied locations as well.

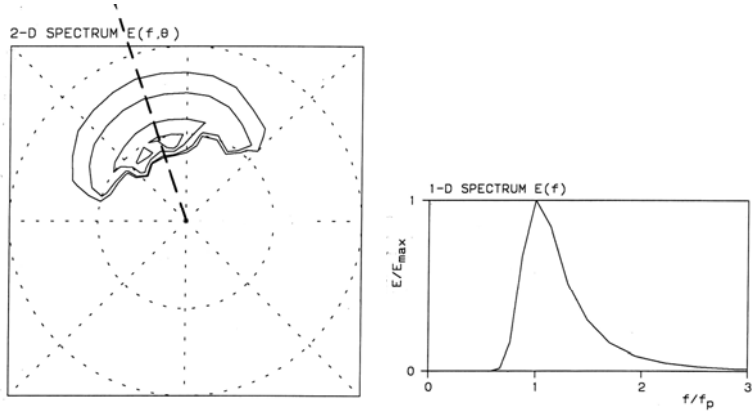


Energy density (wind speed = 19.2m/s and $T$ = 130hrs, energy contour levels [0.1, 0.2, 0.5 and 0.8 $E_{max.}$] [$f_p = 0.078$Hz, $f = 0.10$Hz, $\theta = 343.5^\circ$, $\partial_\theta = 28.1^\circ$]

**Figure 5.1.** Generated wave energy spectrum for observation location no. (1) - Egypt northern coast, "moderate cyclonic pressure conditions".

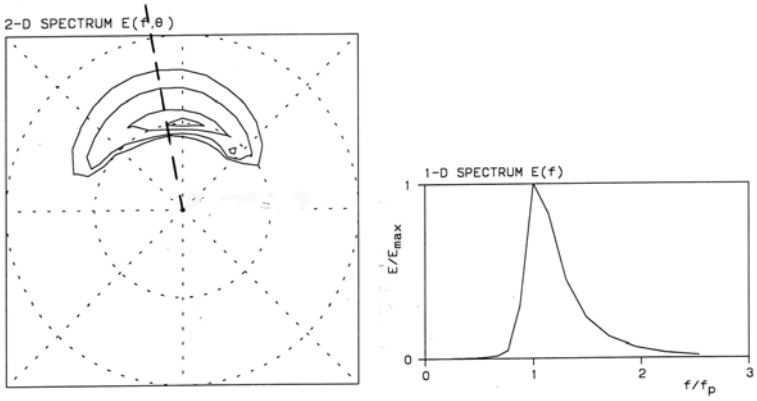


Wind speed = 18.7m/s and T = 130hrs, [energy contour levels 0.1, 0.2, 0.5 and 0.8 $E_{max.}$] [$f_p = 0.197$Hz, $f = 0.143$Hz, $\theta = 350.5^\circ$, $\partial_\theta = 31.2^\circ$]

**Figure 5.2.** Generated wave energy spectrum for observation location number (2) - Egypt northern coast "moderate cyclonic pressure conditions".

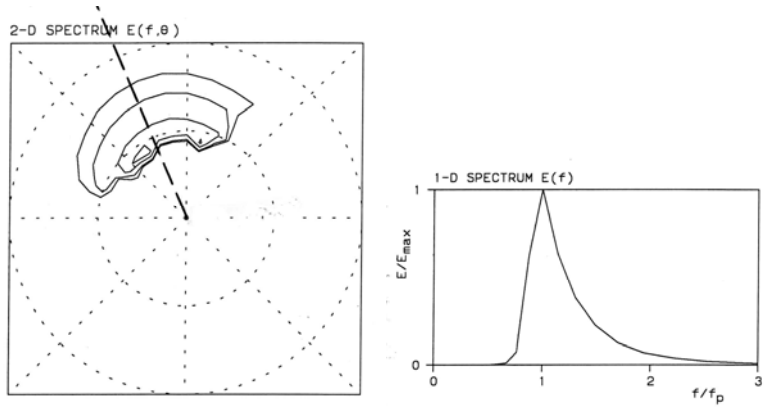


Energy density (wind speed = 20.8m/s and $T$ = 130hrs, [energy contour levels $[0.1, 0.2, 0.5$ and $0.8\ E_{max.}]]$ $[f_p = 0.078\text{Hz}, f = 0.098\text{Hz}, \theta = 340.7^\circ, \partial_\theta = 27.1^\circ]$

**Figure 5.3.** Generated wave energy spectrum for observation location number (3) - Egypt northern coast "moderate cyclonic pressure conditions".

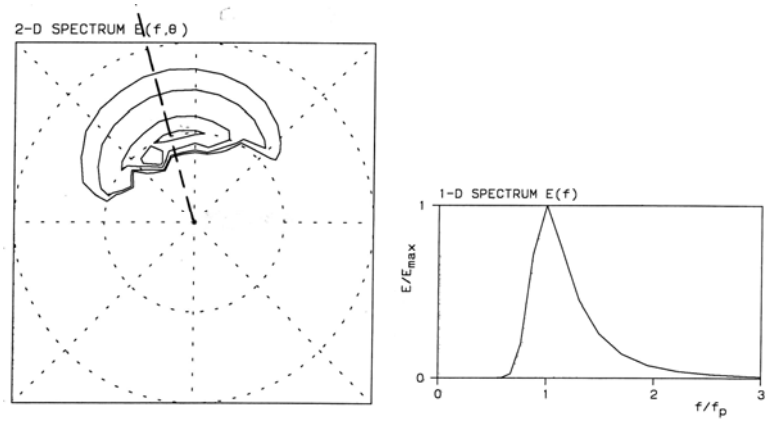


Energy density (wind speed = 19.9m/s and $T$ = 130hrs) [energy contour levels $[0.1, 0.2, 0.5$ and $0.8\ E_{max.}]]$ $[f_p = 0.078\text{Hz}, f = 0.098\text{Hz}, \theta = 345.7^\circ, \partial_\theta = 29.1^\circ]$

**Figure 5.4.** Generated wave energy spectrum for observation location number (4) - Egypt northern coast "moderate cyclonic pressure conditions".

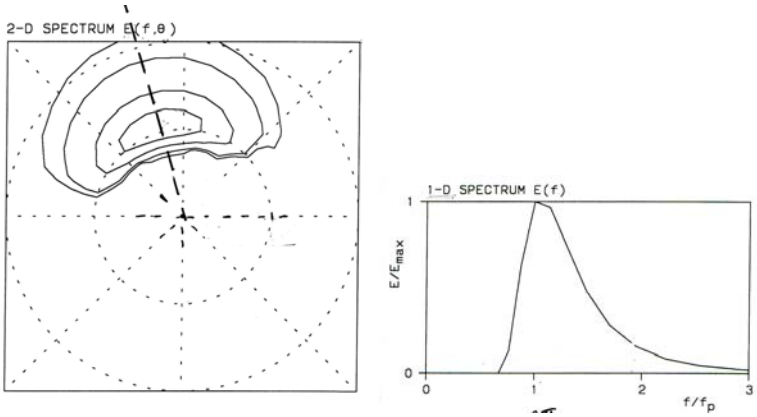


Energy density (wind speed = 10.5m/s and T = 130hrs) [energy contour levels [0.1, 0.2, 0.5 and 0.8 $E_{Max.}$]] [$f_p = 0.116$Hz, $f = 0.159$Hz, $\theta = 345.9^\circ$, $\partial_\theta = 29.2^\circ$]

**Figure 6.1.** Generated wave energy spectrum for observation location number (1) - Egypt northern coast, "high cyclonic pressure conditions".

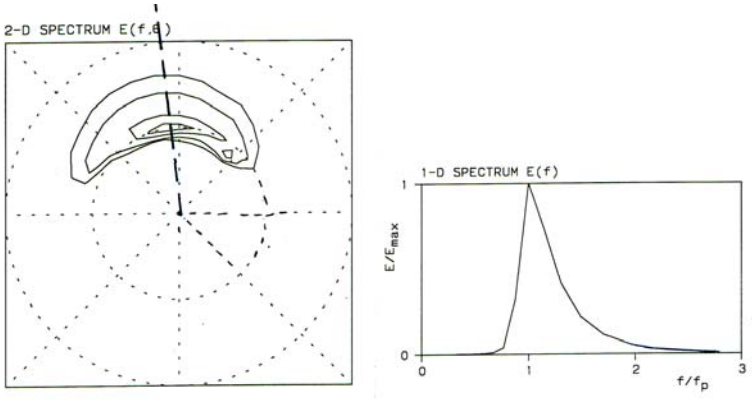


Energy density (wind speed = 10.1 m/s and $T$ = 130 hrs) [energy contour levels [0.1, 0.2, 0.5 and 0.8 $E_{Max.}$]] [$f_p = 0.257$Hz, $f = 0.305$Hz, $\theta = 350.9^\circ$, $\partial_\theta = 31.3^\circ$]

**Figure 6.2.** Generated wave energy spectrum for observation location number (2) - Egypt northern coast, "high cyclonic pressure conditions".

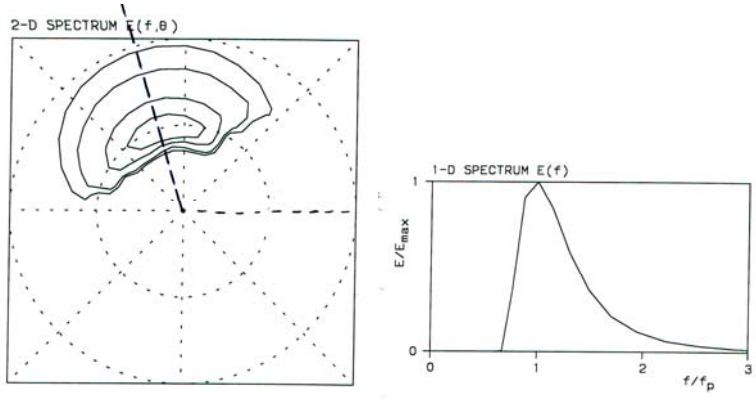


Energy density (wind speed = 11.4 m/s and $T$ = 130 hrs) [energy contour levels [0.1, 0.2, 0.5 and 0.8 $E_{Max.}$] [$f_p = 0.116$Hz, $f = 0.149$Hz, $\theta = 342.5^\circ$, $\partial_\theta = 28.2^\circ$]

**Figure 6.3.** Generated wave energy spectrum for observation location number (3) - Egypt northern coast, "high cyclonic pressure conditions".

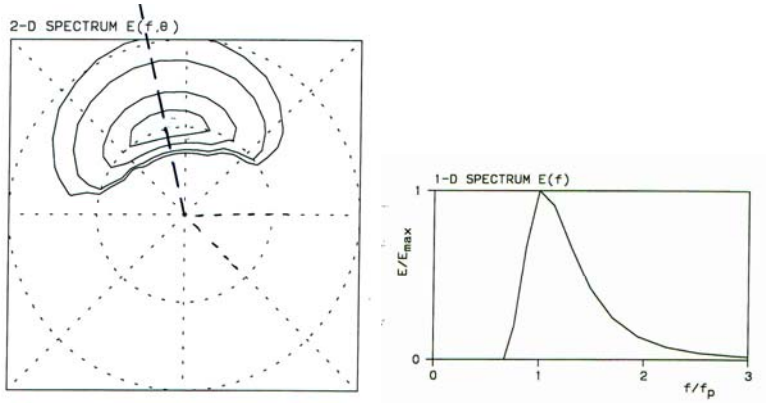


Energy density (wind speed = 10.7 m/s and $T$ = 130 hrs) [energy contour levels [0.1, 0.2, 0.5 and 0.8 $E_{Max.}$]] [$f_p = 0.116$Hz, $f = 0.155$Hz, $\theta = 347.5^\circ$, $\partial_\theta = 30.3^\circ$]

**Figure 6.4.** Generated wave energy spectrum for observation location number (4) - Egypt northern coast, "high cyclonic pressure conditions".

### 4.2. Case study no. (2): closed bay in the southern boundary of the Atlantic Ocean in South America continent

The second case study represents a closed bay in the southern boundary of the

Atlantic Ocean. Figure 7 presents the domain for case no. (2) of a closed bay in the Atlantic Ocean. Figure 8 represents the energy rays for observation location number (5), closed bay in the southern boundary of the Atlantic Ocean. For this case, all fetches are considered limited. To study the effect of the cyclone development on the generated wave energy with time, a cyclone with a total occurrence period of 24 hours was considered (GmbH and Co. KG [16] and NASA [17]). Only one observation location was taken into consideration (location 5). The study followed the cyclone development every two hours, starting with [2 hours] with a time step of two hours as well (12 follow steps were considered). The main inputs for this case are presented as in Appendix (A.4). Figures 9.1 through 9.11 present examples for the generated wave energy spectrum for observation location No. (5), which is located in the southern boundary of the bay.


**Figure 7.** Study domain for case no. (2) closed bay in the Atlantic Ocean "Latin America" (after Google Earth).

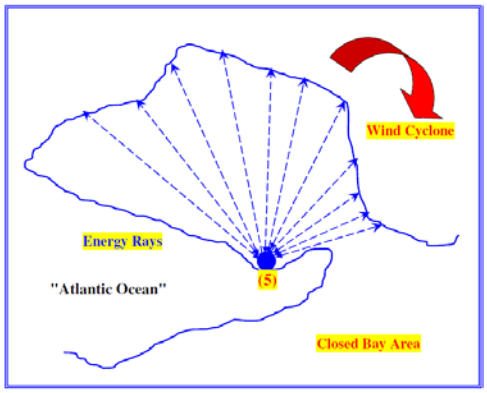


**Figure 8.** Energy rays for observation location number (5) closed bay area-Atlantic Ocean "Latin America".

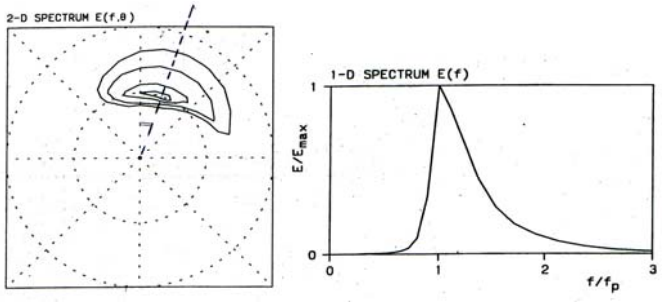


Energy density (wind speed = 24.5 m/s and $T$ = 2 hrs) [energy contour levels [0.1, 0.2, 0.5 and 0.8 $E_{Max.}$] [$f_p = 0.141$Hz, $f = 0.207$Hz, $\theta = 19.4^\circ$, $\partial_\theta = 22.2^\circ$]

**Figure 9.1.** Generated wave energy spectrum for observation location no. (5) - closed bay in the Atlantic Ocean, "after 2 hours".

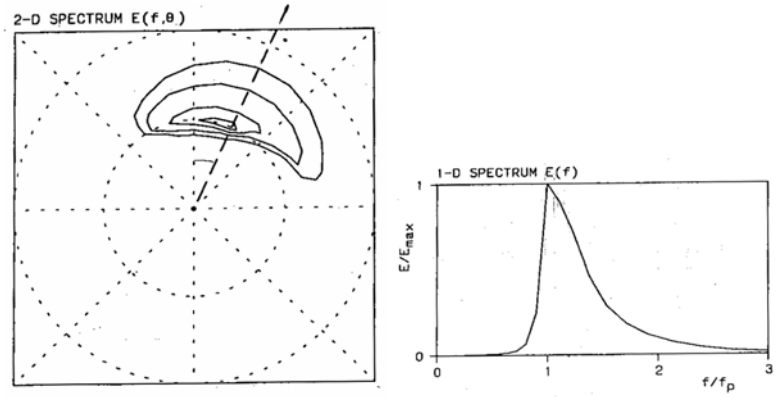


Energy density (wind speed = 23 m/s and $T$ = 4hrs) [energy contour levels [0.1, 0.2, 0.5 and 0.8 $E_{Max.}$]] [$f_p = 0.151$Hz, $f = 0.209$Hz, $\theta = 21.6^\circ$, $\partial_\theta = 27.3^\circ$]

**Figure 9.2.** Generated wave energy spectrum for observation location no. (5) - closed bay in the Atlantic Ocean, "after 4 hours".

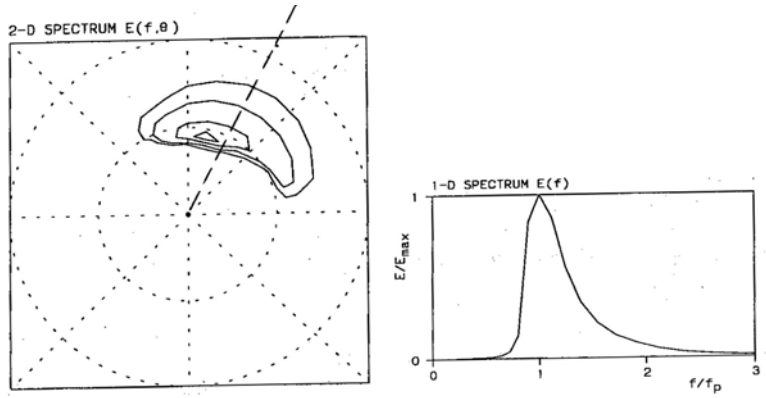


Energy density (wind speed = 21.5 m/s and $T$ = 6 hrs) [energy contour levels $[0.1, 0.2, 0.5$ and $0.8\ E_{Max.}]]$ $[f_p = 0.168\text{Hz}, f = 0.216\text{Hz}, \theta = 27.3^\circ, \partial_\theta = 27.2^\circ]$

**Figure 9.3.** Generated wave energy spectrum for observation location no. (5) - closed bay in the Atlantic Ocean, "after 6 hours".

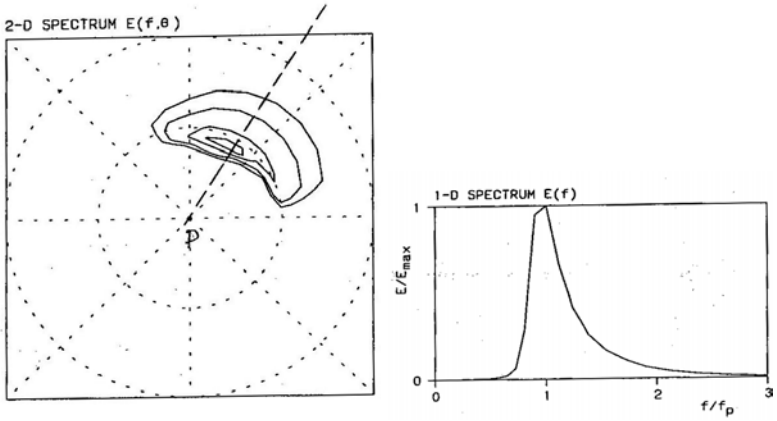


Energy density (wind speed = 19.6 m/s and $T$ = 8 hrs) [energy contour levels $[0.1, 0.2, 0.5$ and $0.8\ E_{Max.}]]$ $[f_p = 0.187\text{Hz}, f = 0.23\text{Hz}, \theta = 35.4^\circ, \partial_\theta = 26.9^\circ]$

**Figure 9.4.** Generated wave energy spectrum for observation location no. (5) - closed bay in the Atlantic Ocean, "after 8 hours".

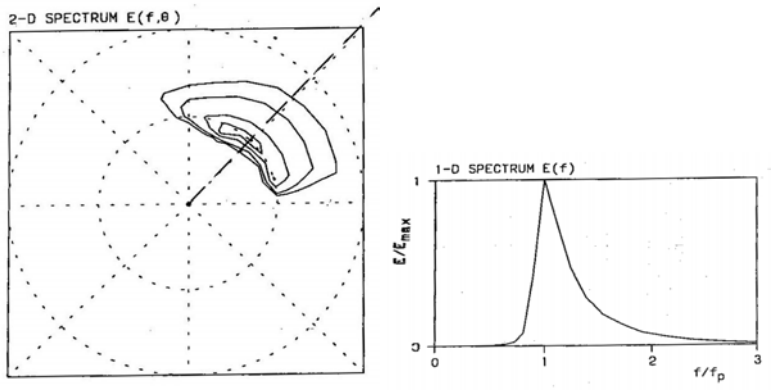


Energy density (wind speed = 17.5 m/s and $T$ = 10 hrs) [energy contour levels $[0.1, 0.2, 0.5$ and $0.8\ E_{Max.}]]$ $[f_p = 0.187\text{Hz}, f = 0.248\text{Hz}, \theta = 44.7^\circ, \partial_\theta = 26.3^\circ]$

**Figure 9.5.** Generated wave energy spectrum for observation location no. (5) - closed bay in the Atlantic Ocean, "after 10 hours".

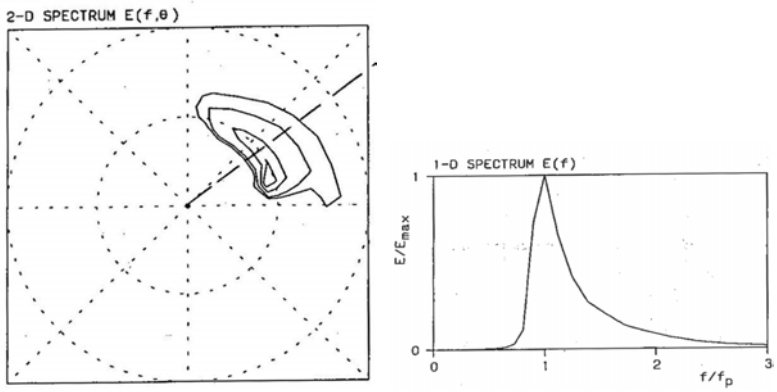


Energy density (wind speed = 16.1 m/s and $T$ = 12 hrs) [energy contour levels $[0.1, 0.2, 0.5$ and $0.8\ E_{Max.}]]$ $[f_p = 0.208\text{Hz}, f = 0.277\text{Hz}, \theta = 56.2^\circ, \partial_\theta = 26^\circ]$

**Figure 9.6.** Generated wave energy spectrum for observation location no. (5) - closed bay in the Atlantic Ocean, "after 12 hours".

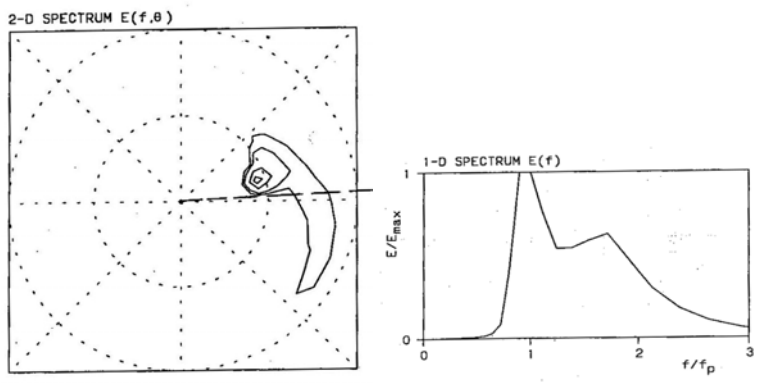


Energy density (wind speed = 17.6 m/s and $T = 16$ hrs) [energy contour levels $[0.1, 0.2, 0.5$ and $0.8\ E_{Max.}]$ $[f_p = 0.232\text{Hz}, f = 0.371\text{Hz}, \theta = 89.6^\circ, \partial_\theta = 32.4^\circ]$

**Figure 9.7.** Generated wave energy spectrum for observation location no. (5) - closed bay in the Atlantic Ocean, "after 16 hours".

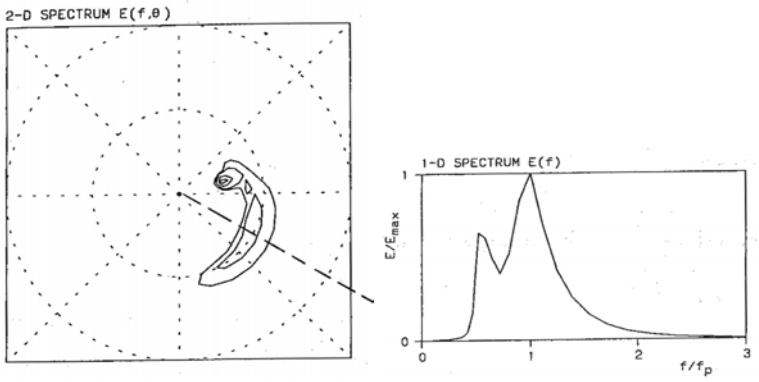


Energy density (wind speed = 19.7 m/s and T = 18 hrs) [energy contour levels $[0.1, 0.2, 0.5$ and $0.8\ E_{Max.}]]$ $[f_p = 0.398\text{Hz}, f = 0.415\text{Hz}, \theta = 111.1^\circ, \partial_\theta = 35.2^\circ]$

**Figure 9.8.** Generated wave energy spectrum for observation location no. (5) - closed bay in the Atlantic Ocean, "after 18 hours".

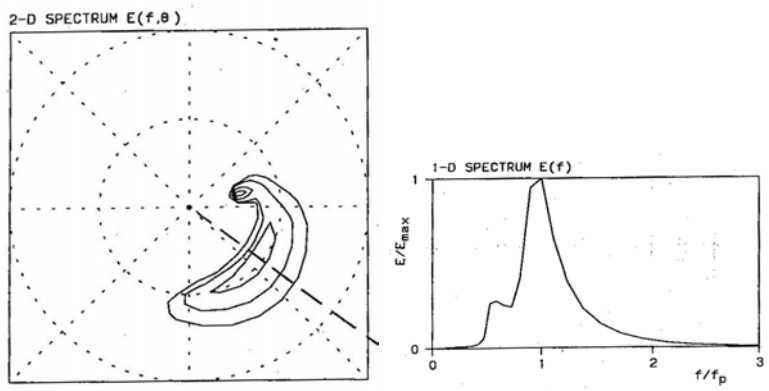


Energy density (wind speed = 21.6 m/s and $T$ = 20 hrs) [energy contour levels $[0.1, 0.2, 0.5$ and $0.8\ E_{Max.}]]$ $[f_p = 0.398\text{Hz}, f = 0.437\text{Hz}, \theta = 128.7^\circ, \partial_\theta = 34^\circ]$

**Figure 9.9.** Generated wave energy spectrum for observation location no. (5) - closed bay in the Atlantic Ocean, "after 20 hours".

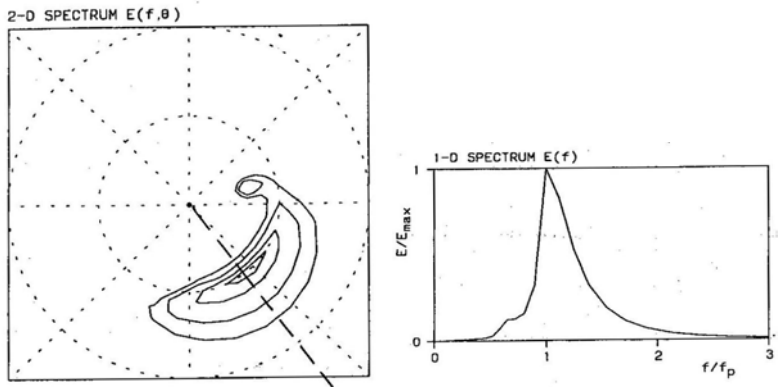


Energy density (wind speed = 23 m/s and $T$ = 22 hrs) [energy contour levels $[0.1, 0.2, 0.5$ and $0.8\ E_{Max.}]]$ $[f_p = 0.357\text{Hz}, f = 0.444\text{Hz}, \theta = 140.7^\circ, \partial_\theta = 31.7^\circ]$

**Figure 9.10.** Generated wave energy spectrum for observation location no. (5) - closed bay in the Atlantic Ocean, "after 22 hours".

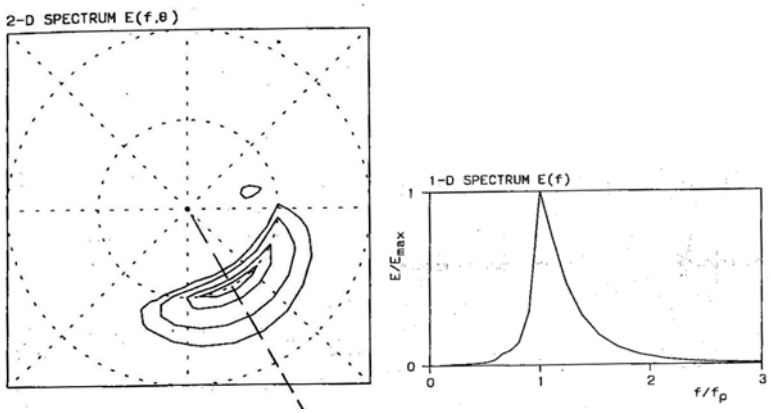


Energy density (wind speed = 23.9 m/s and $T$ = 24 hrs) [energy contour levels $[0.1, 0.2, 0.5$ and $0.8\ E_{Max.}]]$ $[f_p = 0.357\text{Hz}, f = 0.445\text{Hz}, \theta = 148^\circ, \partial_\theta = 30^\circ]$

**Figure 9.11.** Generated wave energy spectrum for observation location no. (5) - closed bay in the Atlantic Ocean, "after 24 hours".

This case study showed in a clear form the manner of the cyclone development on the generated energy. With cyclone development in time, the generated wave energy decayed. The maximum generated energy came after two hours and the minimum one came after sixteen to eighteen hours from the beginning of the cyclone. After, two hours at 20 hours occurrence, the generated wave energy started to grow again to be close to the generated one at the cyclone beginning. During the cyclone turn, the effective fetch lengths vary and so the generated energy. For the first fourteen hours from the cyclone generation, the angle of directional spreading $(\partial\theta)$ is considered close $(\partial\theta = 26.4^\circ$ and $27.9^\circ)$. Same condition for it in the cyclone development period starting from 16 hours till the end of twenty four hours $(\partial\theta = 32.4^\circ$ and $30^\circ)$. For the wave propagation angle $(\theta)$, it varies from north (N) and south (S) within a wide sector close to 130 degree $(\text{from } \theta = 19.4^\circ \text{ to } 148^\circ)$.

## 5. Conclusions

From the results of the handled two case studies for both the Egyptian northern coast on the Mediterranean Sea and a closed bay area on the southern boundary of the Atlantic Ocean in South America continent as cases with different boundary

conditions, the study came up with a group of conclusions as follows:

- The generated wave energy distributions for the coastal stretches with quite open boundaries and straight coastline (as the case of the Egyptian northern coast on the Mediterranean Sea) are considered quite close in both form and quantity. This comes based on the close boundary conditions. The high pressure generates more wave energy based on the wind cyclonic effect. For this case study, both the wave propagation angle $(\theta)$ and the angle of wave directional spreading $(\partial\theta)$ become quite close for the different observation locations through the simulation time of the cyclonic effect.

- For the closed bays case (with small opening in comparison to the bay dimensions), the cyclonic effect varies with the development in the simulated time for the same observation location. This variation effect comes clear in both wave propagation angle $(\theta)$ and angle of wave directional spreading $(\partial\theta)$. This occurs as they vary with time progress of the cyclonic effect development. Similar conditions may also occur for some certain simulated periods and so the energy development progress accompanying to the cyclonic activity effects.

The (1-D) wave spectrum may appear with two peaks, see Figures 9.7 and 9.8. It may represent two different wave fields (wind sea and swell waves). On the other hand, they can represent both old and new waves as the wind changes its direction, so the first is the old traces of energy and the second represents the generated energy from a recent wind field.

- Long fetches cause an effect represented in more generated energy for the wind generated waves. With the fetch growth, the spectrum shape may become more flat.

**Acknowledgements**

Thanks to **ALLAH** for the power and the knowledge. Deep thanks to my family for the continuous encouragement. Deep gratitude to my professors, who gave me the favor of learning the coastal engineering subjects in a profesional outframe.

## Appendices A. Main Inputs for Handled Case Studies

### A.1. Main inputs for DOLPHIN-B1 model (student version)

- Project name of the studied project.

- Coordinates of the observation points (spherical coordinates as longitudinal and latitudinal coordinates).

- Units for distance and time (km & hr).
- Time step used for computation (1hr).
- Wind field type: (uniform/variable).
- Wind speed (default - km/hr).
- Wind propagation direction (deg.), (eg., 0 = wind coming from north).
- Coastline profile, used default coastline profile files for known areas around the world (eg., The Mediterranean Sea).
- Lowest $(F_L)$ and Highest frequency $(F_H)$, DOLPHIN-B1 calculates the wave energy density between these two given frequencies through a given number of steps.
- Angle of energy propagation = from 0 to 360 degree (37 Sectors).

**A.2. Main inputs for the high pressure cyclone of Case (1) - "Egypt northern coast"** (Ministry of transport-Egypt [18]) and (Admiralty Publications [19])**.**

Project 'Storm on the Egyptian coast'

coordinate spherical

units km hr

spectrum 20 , 0.04, 0.5, 37

cyclone mbar

0., 100., 50., 320., 320.

130., 80., 40., 280., 290.

wind variable ' ', 20., 10., 10., 10., 10., 6., 25., 35.

location 'p1' 32.3, 31.4, 90.

'p2' 30.0, 31.1, 100.

'p3' 34.0, 31.4, 110.

'p4' 30.4, 31.5, 120.

**A.3. Main inputs for the high pressure cyclone of Case (1) - "Egypt northern coast"** (Ministry of transport-Egypt [18]) and (Admiralty Publications [19])**.**

Cyclone mbar

0., −65.2, −42.7, 80., 30.

130., 63.9, −42.7, 80., 30.

***** *The rest is similar to case* (A .1).

**A.4. Main inputs for the high pressure cyclone of Case (2) - "Closed bay in the Atlantic Ocean, Latin America"** (GmbH & Co. KG [16]) and (NASA [17]).

Project Closed Bay – Atlantic Ocean'

coordinate spherical

units km hr

spectrum 40, 0.03, 2, 30

cyclone mbar

0., –65.2., –42.7, 80., 30.

24., –63.9, –42.7, 80., 30.

location 'p1' –64.5, –42.94, 2.

'p2' –64.5, –42.94, 4.

'p3' –64.5, –42.94, 6.

'p4' –64.5, –42.94, 8.

'p5' –64.5, –42.94, 10.

'p6' –64.5, –42.94, 12.

'p7' –64.5, –42.94, 14.

'p8' –64.5, –42.94, 16.

'p9' –64.5, –42.94, 18.

'p10' –64.5, –42.94, 20.

'p11' –64.5, –42.94, 22.

'p12' –64.5, –42.94, 24.

## References

[1] K. Hasselmann, On the non-linear energy transfer in a gravity-wave spectrum, I, General Theory, J. Fluid. Mech. 12 (1962), 481-500.

[2] CERC-Coastal Engineering Research Center, Shore Protection Manual, Washington, DC: US Army Corps of Engineers 2(4) (1984), 1-487.

[3] CERC-Coastal Engineering Research Center, Coastal Engineering Manual, CERC (Coastal Engineering Research Center, http://www.scribd.com/doc/15187705/Coastal-Engineering-Manual-Part-II-Chapter-1 (2002). (accessed: Aug., 2010).

[4] J. Darbyshire, Prediction of wave characteristics over the North Atlantic, J. Inst. Navigation 14 (1961), 339-347.

[5] M. S. Longuet-Higgins, On the joint distribution of the periods and amplitudes of sea waves, J. Geophys. Res. 80 (1975), 2688-2694.

[6] Wikimedia Foundation Inc., The free encyclopedia, Cyclone, http://en.wikipedia.org /wiki/Cyclone (2010) (accessed: Sept.-2010).

[7] G. J. Komen, Dynamics and Modeling of Ocean Waves, Cambridge University Press, New York, 1994.

[8] Y. Goda, Numerical experiments on waves statistics with spectral simulation, Report, Port and Harbour Res. Inst. (Japan) 9 (1970), 3-57.

[9] Digital Hydraulics B. V. DOLPHIN-B1 user manual, Student Version 30.27, The Netherlands, 1997.

[10] R. J. Seymour, Estimating wave generation on restricted fetches, Proc. ASCE J. of Waterway Port, Coastal and Ocean Div. 103(2) (1977), 251-264.

[11] G. Ph. van Vledder, Extension of the discrete interaction approximation for computing nonlinear quadruplet wave-wave interactions in operational wave models, In: 4th ASCE International Symposium Ocean Waves, Meas. Anal., San Francisco, California, USA, 2001, pp. 540-549.

[12] H. S. Robert, Department of Oceanography, Texas A & M University Introduction to Physical Oceanography: Chapter 16-Ocean Waves http://oceanworld.tamu.edu/ resources/ocng_textbook/chapter16/chapte (2006) (accessed: Aug. 2010).

[13] S. Narasimhan and M. C. Deo, Spectral analysis of waves-a study, Proc. Civil Engineering in the Oceans IV Conference, San Francisco 2 (1979), 877-892.

[14] R. H. Stewart, Introduction to Physical Oceanography, Department of Oceanography, Texas A & M University http://oceanworld.tamu.edu/resources/ocng_textbook/ chapter16 /chapter16_04.htm (2006). (accessed: Aug. 2010).

[15] K. V. Thomas, M. Baba and C. M. Harish, Wave groupiness in long travelled swell, J. Waterway, Port Coastal Ocean Eng. 112 (1986), 498-511.

[16] H. Gmb and K. G. Co, http://www.windfinder.com/windreports/windkarte_ argentina.htm, Germany (2010) (accessed: Sept.-2010).

[17] NASA National Aeronautics and Space Administration. http://worldwind.arc.nasa.gov. (2010) (Accessed: Sept.-2010).

[18] Ministry of transport-Egypt. Climatological Atlas of Egypt. (1996).

[19] Admiralty Publications, Mediterranean Pilot, NP46. Somerset, UK: Admiralty Publications, Hydrographic Department, 2000, pp. 15-36.